

Identification of circRNA-miRNA-mRNA network as biomarkers for interstitial cystitis/bladder pain syndrome

Shi-Qin Yang^{1,*}, Liao Peng^{1,*}, Le-De Lin¹, Yuan-Zhuo Chen¹, Meng-Zhu Liu¹, Chi Zhang¹, Jia-Wei Chen¹, De-Yi Luo¹

¹Department of Urology, Institute of Urology, West China Hospital, Sichuan University, Chengdu, Sichuan 610041, P.R. China

*Equal contribution

Correspondence to: De-Yi Luo; email: luodeyi@scu.edu.cn

Keywords: CircRNA, miRNA, circRNA-miRNA-mRNA network, circ.5863, interstitial cystitis

Received: August 7, 2023

Accepted: October 8, 2023

Published: November 2, 2023

Copyright: © 2023 Yang et al. This is an open access article distributed under the terms of the [Creative Commons Attribution License](https://creativecommons.org/licenses/by/4.0/) (CC BY 4.0), which permits unrestricted use, distribution, and reproduction in any medium, provided the original author and source are credited.

ABSTRACT

Interstitial cystitis/bladder pain syndrome (IC/BPS) is a long-lasting and incapacitating disease, and the exact factors that affect its onset and advancement are still uncertain. Thus, the main aim was to explore new biomarkers and possible therapeutic targets for IC/BPS. Next-generation high-throughput sequencing experiments were performed on bladder tissues. Based on the interactions between circRNA and miRNA, as well as miRNA and mRNA, candidates were selected to build a network of circRNA-miRNA-mRNA. The STRING database and Cytoscape software were utilized to build a protein-protein interaction (PPI) network to pinpoint the hub genes associated with IC/BPS. The expression levels of circRNA and miRNA in the network were confirmed through quantitative polymerase chain reaction. Western blot was applied to confirm the stability of the lipopolysaccharide-induced IC/BPS model, and the effect of overexpression of circ.5863 by lentivirus on inflammation. Ten circRNA-miRNA interactions involving three circRNAs and six miRNAs were identified, and IFIT3 and RSAD2 were identified as hub genes in the resulting PPI network with 19 nodes. Circ.5863 showed a statistically significant decrease in the constructed model, which is consistent with the sequencing results, and overexpression via lentiviral transfection of circ.5863 was found to alleviate inflammation damage. In this study, a circRNA-miRNA-mRNA network was successfully constructed, and IFIT3 and RSAD2 were identified as hub genes. Our findings suggest that circ.5863 can mitigate inflammation damage in IC/BPS. The identified marker genes may serve as valuable targets for future research aimed at developing diagnostic tools and more effective therapies for IC/BPS.

INTRODUCTION

Interstitial cystitis/bladder pain syndrome (IC/BPS) represents a long-lasting and incapacitating condition that severely affects the standard of living of those affected, yet its etiology remains unknown [1]. IC/BPS is estimated to affect a percentage ranging from 0.01% to 6.5% of the general population, with a higher incidence in women [2]. Unfortunately, the diagnosis and treatment of IC/BPS are hindered by our limited understanding of its etiology and pathophysiology [3]. Therefore, it is crucial to investigate the molecular

mechanisms behind IC/BPS to develop accurate diagnostic criteria and effective therapeutic strategies.

Circular RNA (circRNA) is an endogenous non-coding RNA that possesses a distinctive covalently closed loop structure lacking both a 5' cap and a poly(A) tail at its 3' ends [4]. CircRNA is expressed in a variety of mammalian tissues, including serum and tumor tissues [5, 6], and acts as a molecular sponge to effectively bind and suppress miRNA expression [7, 8]. By modulating downstream gene expression through this mechanism, circRNA can exert a pivotal role in the pathogenesis of

various diseases [9]. A recent research [10] has shown that circRNA promotes IC/BPS cell proliferation, migration, epithelial-mesenchymal transition (EMT), and inflammation by regulating miRNA expression. Thus, targeting circRNA may represent a promising therapeutic approach for IC/BPS. Nevertheless, the contribution of other circRNAs, miRNAs, and their underlying functions in the development of IC/BPS are still not completely comprehended.

To address this gap in knowledge, we have sequenced bladder samples from IC/BPS patients and non-IC/BPS patients to identify CircRNAs, miRNAs, and mRNAs exhibiting differential expression (DEcircRNAs, DEmiRNAs, and DEMRNAs, respectively). Our aim is to propose a novel diagnostic and therapeutic strategy for IC/BPS, as there are currently only a few studies [10–12] investigating the role of circRNA or miRNA in this condition, and none that have collected

samples from IC/BPS patients for high-throughput sequencing.

RESULTS

Identification of DEcircRNAs, DEmiRNAs and DEMRNAs

According to the predetermined threshold ($|\log_2FC| \geq 2.0$ and adjusted P value < 0.05), comparisons were made between samples from patients with IC/BPS and samples from patients with pure stress urinary incontinence (PSUI). As a result, 94 DEcircRNAs (45 upregulated and 49 downregulated), 92 DEmiRNAs (74 upregulated and 18 downregulated) and 3103 DEMRNAs (2296 upregulated and 807 downregulated) were identified. Subsequently, the heat map and volcano plots representing the DEcircRNAs, DEmiRNAs, and DEMRNAs are depicted in Figure 1.

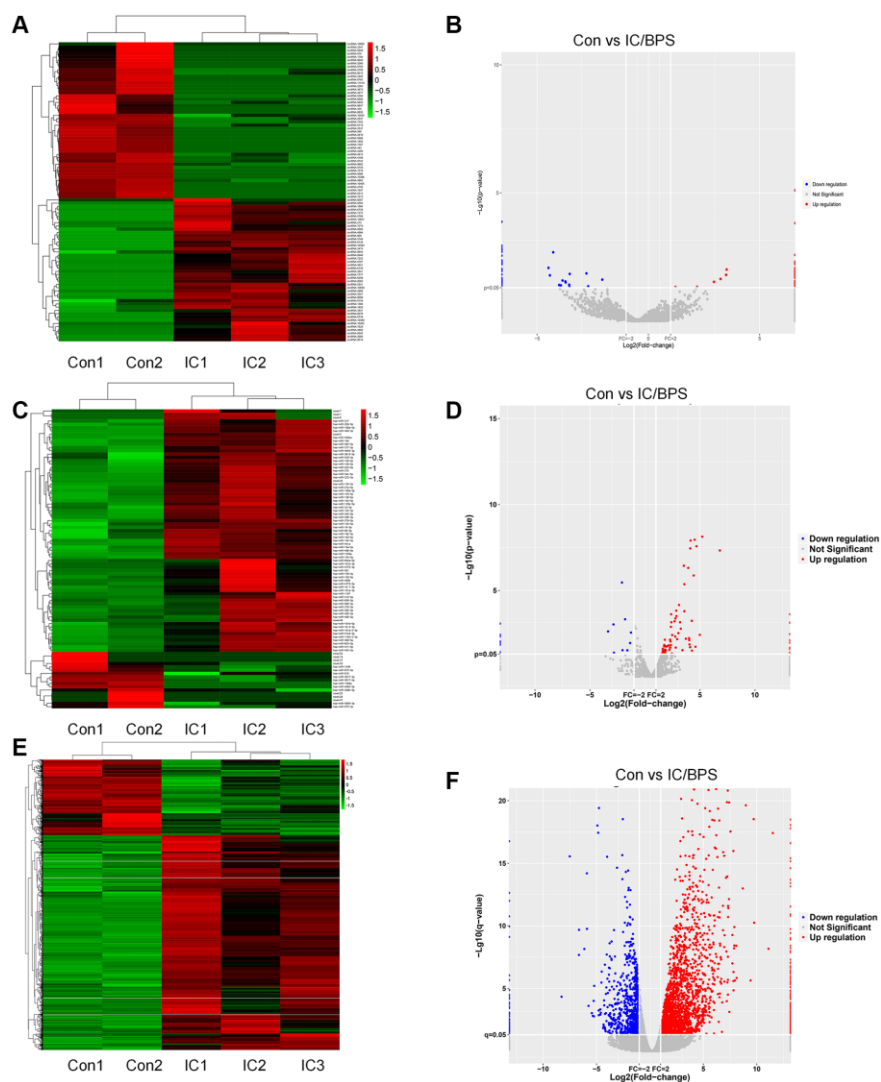


Figure 1. Heatmaps and volcano plots of DEcircRNAs, DEmiRNAs and DEMRNAs in IC/BPS. (A, B) Heatmaps and volcano plots of DEcircRNAs. (C, D) Heatmaps and volcano plots of DEmiRNAs. (E, F) Heatmaps and volcano plots of DEMRNAs.

GO term and KEGG pathways enrichment analysis

Initially, the results of functional enrichment analysis revealed crucial associations of the DEcircRNAs parental genes with pathways related to the apical junction complex, cell-substrate adhesion, and adherens junction (Figure 2A, 2B).

In addition, GO enrichment analysis of DEMiRNAs target genes revealed that the RISC-loading complex is the main cellular component, and protein phosphatase type 1 regular activity is the main molecular function. Besides, the KEGG pathway analysis demonstrated significant enrichment of the DEMiRNAs in the AMPK signaling pathway (Figure 2C, 2D).

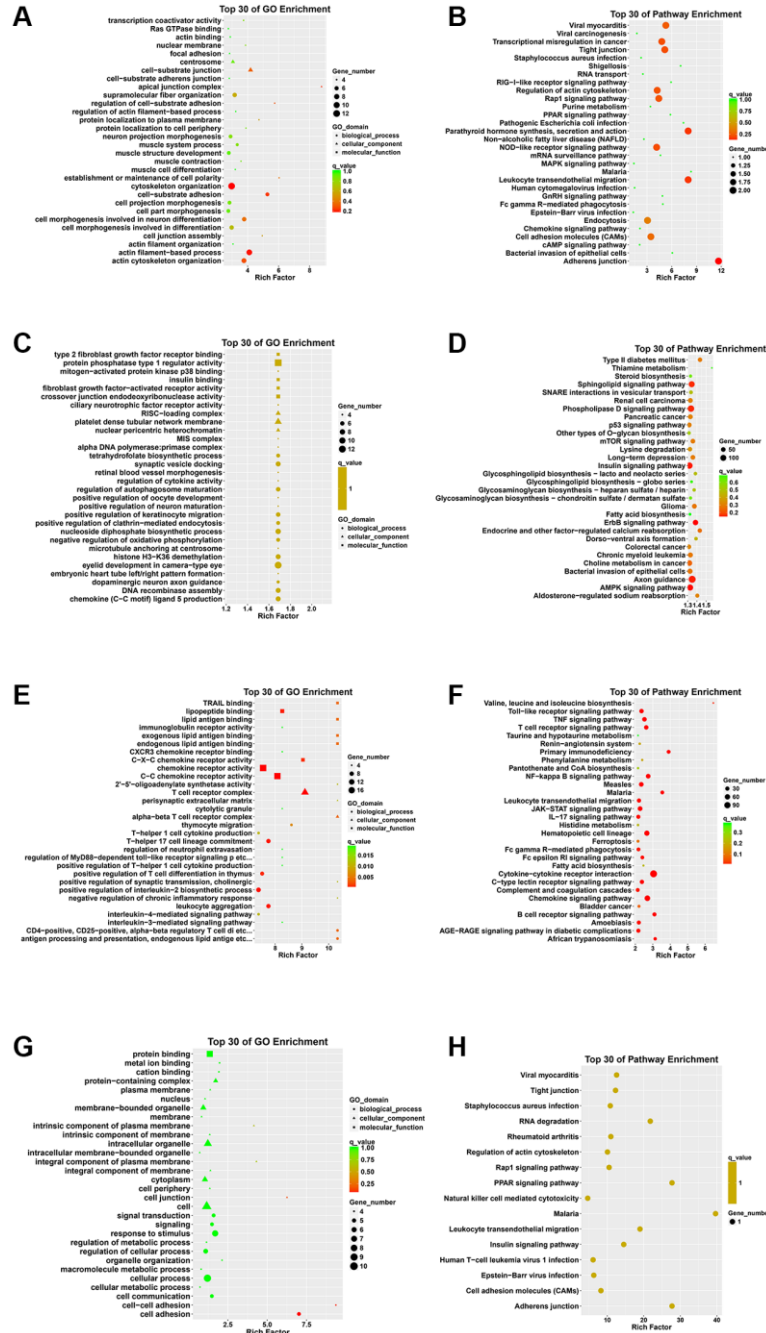


Figure 2. GO annotation and KEGG pathway analysis of DEcircRNA parental genes, DEMiRNA target genes, DEMiRNAs, and genes that intersect DEcircRNA parental genes with DEMiRNAs. (A) Top 30 enriched GO terms of the DEcircRNA parental genes. (B) Top 30 enriched KEGG pathways of the DEcircRNA parental genes. (C) Top 30 enriched GO terms of the DEMiRNA target genes. (D) Top 30 enriched KEGG pathways of the DEMiRNA target genes. (E) Top 30 enriched GO terms of the DEMiRNAs. (F) Top 30 enriched KEGG pathways of the DEMiRNAs. (G) Top 30 enriched GO terms of genes that intersect DEcircRNA parental genes with DEMiRNAs. (H) Top 30 enriched KEGG pathways of genes that intersect DEcircRNA parental genes with DEMiRNAs.

Moreover, the enrichment analysis of the DEMRNAs revealed prominent GO terms such as T cell receptor complex and chemokine receptor activity. Additionally, the KEGG pathway analysis highlighted significant involvement in pathways such as T cell receptor signaling pathway, Toll-like receptor signaling pathway and Cytokine-cytokine receptor interaction (Figure 2E, 2F).

Then, we performed GO analysis on the genes that intersect DEcirRNAs parental gene with the DEMRNAs. Regarding the biological process (BP) aspect, the overlapping genes exhibited significant enrichment in the process of cell adhesion. Cellular processes and response to stimuli were also notable. Additionally, several enriched terms linked to molecular functions, such as protein binding and metal ion binding, were identified. Furthermore, our attention was directed towards the enriched cellular component terms, such as intracellular organelle and cell junction. Moreover, the KEGG pathway analysis revealed significant

enrichment of the overlapping genes in adherens junction and tight junction pathways (Figure 2G, 2H).

Establishment of the circRNA –miRNA –mRNA network

The online CircInteractome database was employed to predict the corresponding circRNAs of the DEMiRNAs, enabling the investigation of their possible functional roles in interstitial cystitis. Upon intersecting with the DEcirRNAs, a total of 10 interactions between circRNAs and miRNAs were identified, involving three circRNAs and six miRNAs. By combining the predicted mRNAs of these six miRNAs from the miRanda databases with the DEMRNAs, we obtained a set of 52 target mRNAs. Ultimately, a circRNA-miRNA-mRNA network was constructed by integrating three overlapping circRNAs, six miRNAs, and 52 target mRNAs (Figure 3). Detailed information regarding these three DEcirRNAs can be found in Table 1.

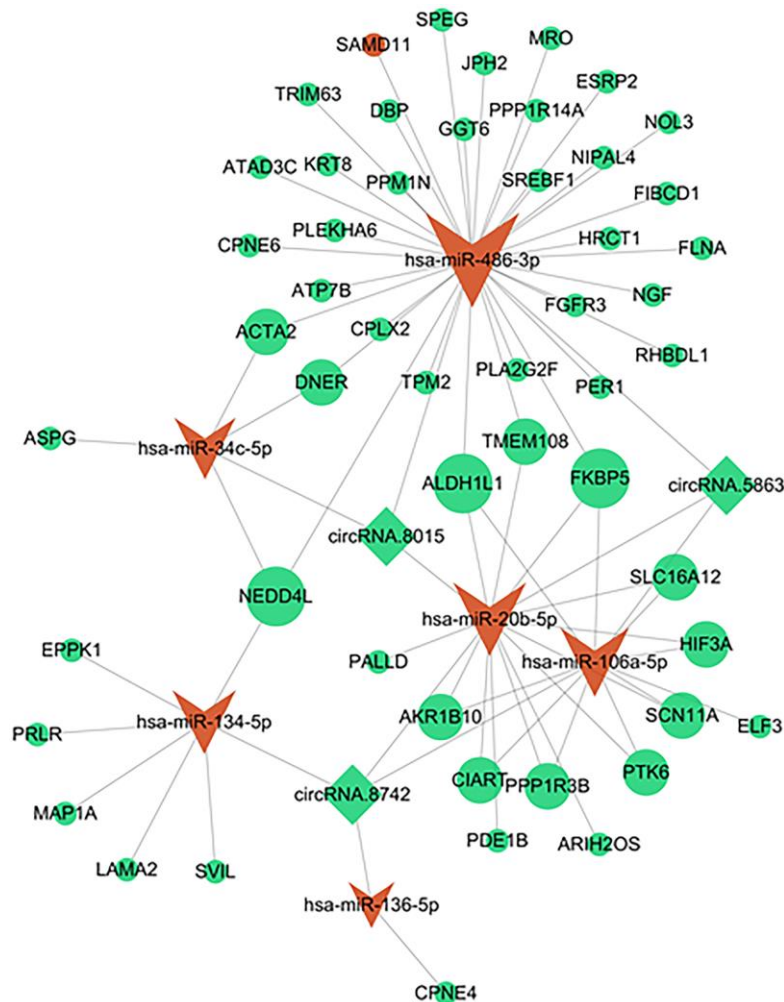


Figure 3. A circRNA-miRNA-mRNA network in IC/BPS. The shape of rhombus represents miRNA, V represents miRNAs, and ellipse represents mRNA. Green represents down regulation and red represents up regulation.

Table 1. Basic information of the 3 DEcircRNAs.

circRNA_id	Position	Genomic Length	Gene symbol	Regulation
circRNA.5863	Chr22:31097269-31104387	7118	SMTN	Down
circRNA.8015	Chr4:38051899-38103157	51258	TBC1D1	Down
circRNA.8742	Chr5:88282042-88292643	10601	TMEM161B-AS1	Down

Establishment of PPI network and identification of hub genes

The PPI network, consisting of 19 nodes, was constructed utilizing the STRING database (Figure 4). Subsequently, the cytoHubba app was employed to identify hub genes, resulting in the identification of IFIT3 and RSAD2 as the hub genes.

Construction of IC/BPS model

Following the outlined methodology, an IC/BPS model was established. The Western blotting and q-PCR analyses demonstrated reduced expression levels of barrier function markers (E-Cadherin and ZO-1) and elevated expression levels of inflammatory markers (IL-1 β , IL-6, and TNF- α). These results indicate the reliability of our modeling (Figure 5).

Identification of CircRNA, miRNA in IC/BPS models

To validate our sequencing findings, we performed qPCR validation of the circRNA and miRNA in the

network that was constructed in the IC/BPS model. Our qPCR results were in agreement with the sequencing data, demonstrating a significant downregulation of circ.5863 and a significant upregulation of hsa-miR-486-3p and hsa-miR-20b-5p expression levels (Figure 6).

CircRNA inhibits cell inflammation in HUCs

To examine the role of circRNA in the progression of IC/BPS, lentivirus-mediated transduction was employed to achieve stable overexpression of circ.5863 in HUCs. The findings from Western blotting and qPCR suggest that overexpression of circ.5863 can significantly downregulate the levels of IL-6, IL-1 β , and TNF- α expression, although there was no significant change in barrier indicators (E-cadherin and ZO-1). The results of both methods are consistent with each other (Figure 7).

DISCUSSION

IC/BPS is a multifaceted disease with heterogeneous medical presentations and elusive etiology [13]. The precise pathogenesis of IC/BPS remains uncertain, but the

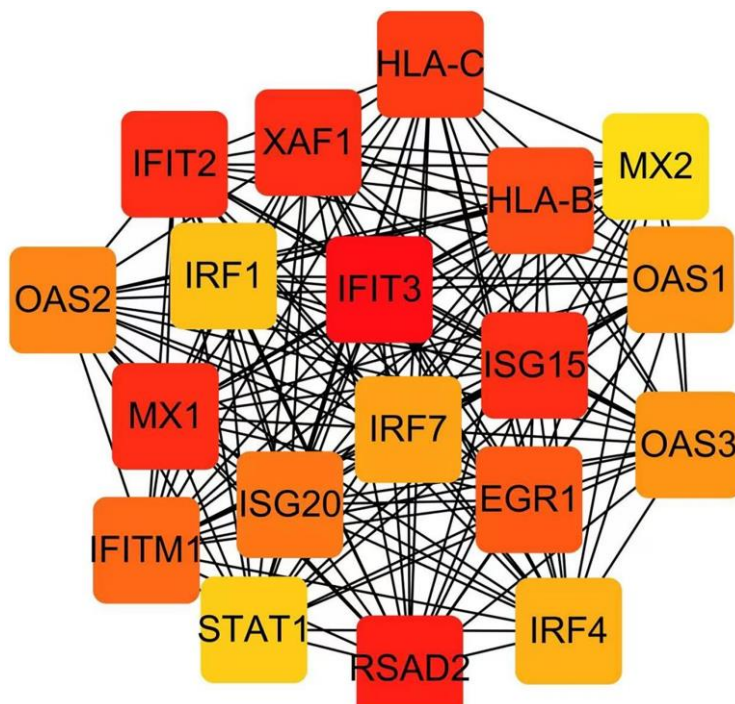


Figure 4. Identification of hub genes in the PPI network with the Cytoscape plugin cytoHubba.

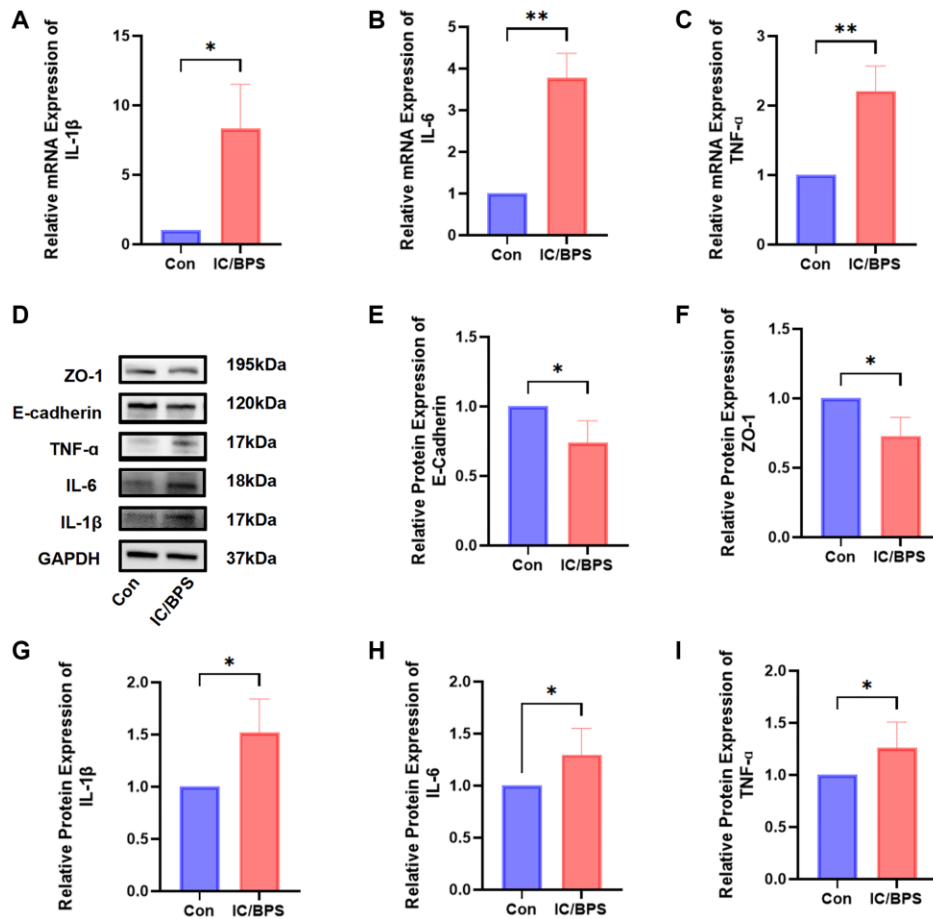


Figure 5. The construction of an IC/BPS model. (A–C) The qPCR showed that the expression levels of IL-1 β , IL-6, and TNF- α were significantly higher in the lipopolysaccharide-induced IC/BPS model compared to Con. (D) Western blot analysis of ZO-1, E-cadherin, IL-1 β , IL-6, TNF- α . (E–I) Relative protein expression of E-cadherin, ZO-1, IL-1 β , IL-6, TNF- α . Results were presented as mean \pm SD. * P < 0.05, ** P < 0.01. All of the experiments were performed in triplicate.

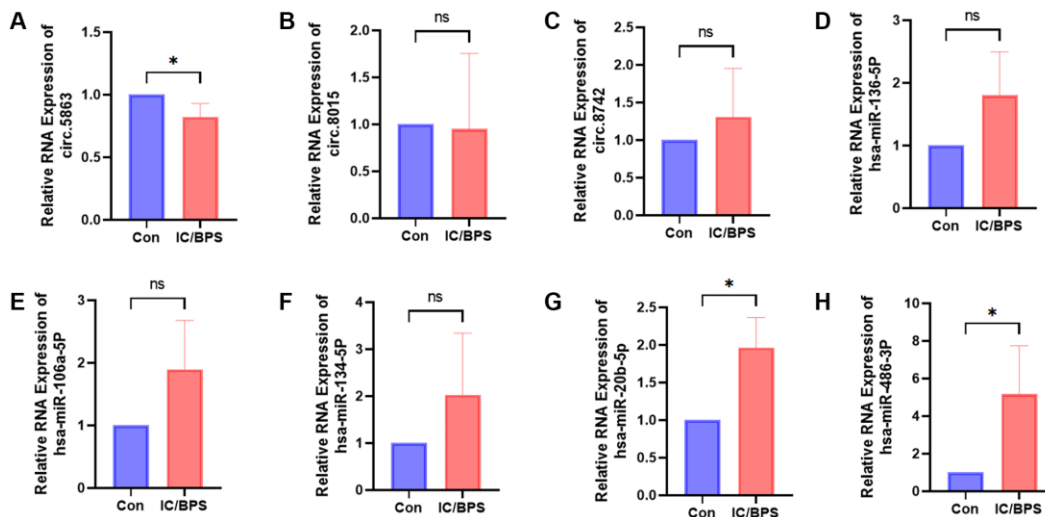


Figure 6. The relative RNA expression of circRNAs and miRNAs identified in the sequencing-constructed circRNA-miRNA-mRNA network was validated in the lipopolysaccharide-induced IC/BPS model. (A–H) The relative RNA expression of circ.5863, circ.8015, circ.8742, hsa-miR-136-5p, hsa-miR-106a-5p, hsa-miR-134-5p, hsa-miR-20b-5p, hsa-miR-486-3p. Results were presented as mean \pm SD. * P < 0.05. All of the experiments were performed in triplicate. "Con" refers to the normal HUCs control group, while "IC/BPS" refers to the LPS-induced IC/BPS model group.

aggregation of inflammatory cells and the disruption of barrier function are widely recognized as important pathological features [14]. IC/BPS is currently diagnosed mainly by exclusion, and no complete cure is available. Thus, there is an immediate necessity to search for novel biomarkers for diagnosis and treatment.

CircRNA represents a distinctive class of RNA with a circular structure that makes it more stable and resistant to RNA exonuclease than linear RNA [15]. Researchers have linked circRNA to various diseases, including neurological disorders [16], coronary artery disease [17], and cancers [18], by acting

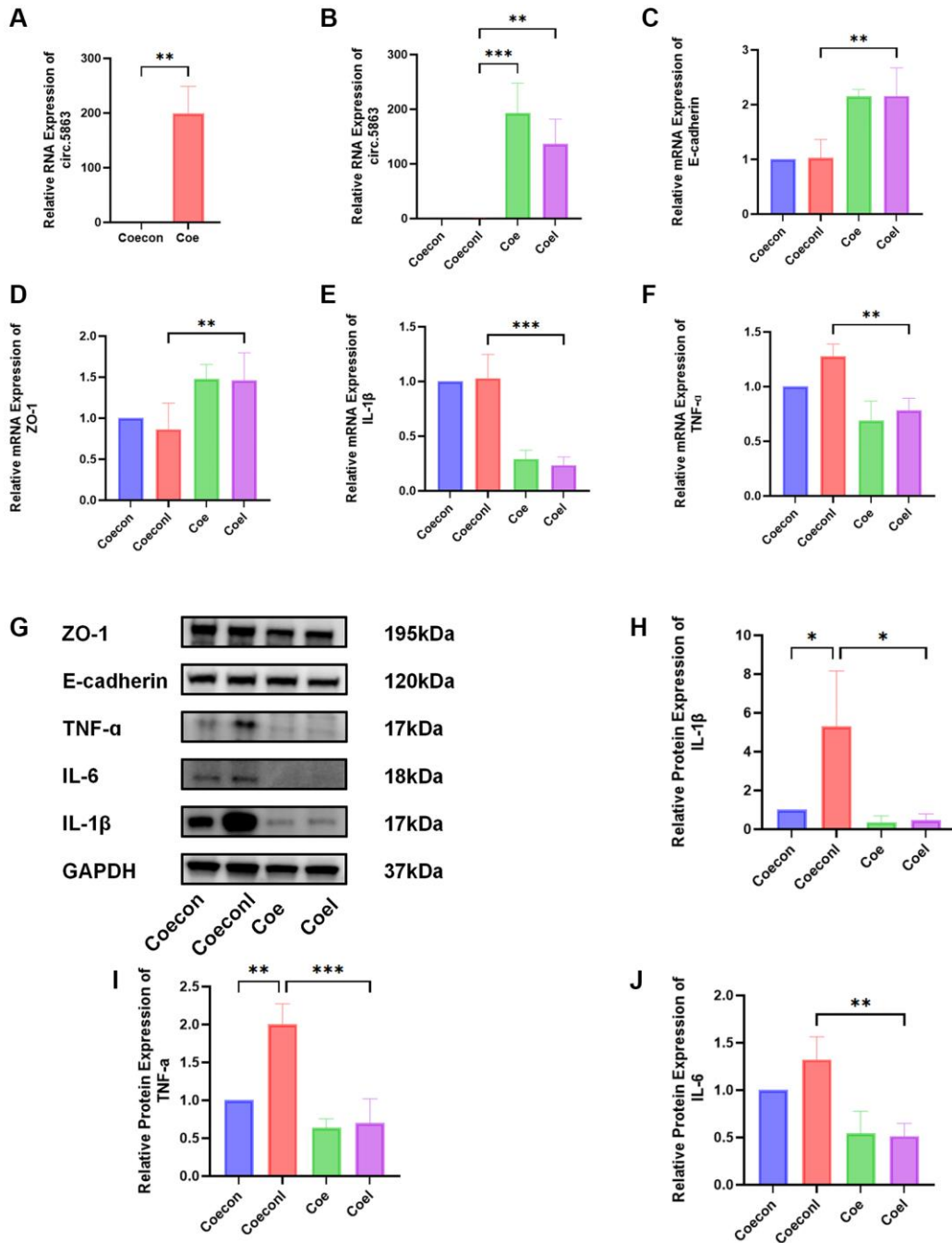


Figure 7. Overexpression of circ.5863 through lentiviral transfection can alleviate inflammation in IC/BPS. (A) qPCR validation of overexpression of circ.5863. (B–F) The qPCR results from relative quantitative analysis showed that overexpression of circ.5863 can restore barrier function and reduce the expression levels of IL-1β, and TNF-α. (G–J) The Western blot results and relative protein quantification analysis showed that overexpression of circ.5863 can reduce the levels of IL-1β, IL-6, and TNF-α. Results were presented as mean ± SD. * $P < 0.05$, ** $P < 0.01$, *** $P < 0.001$. All of the experiments were performed in triplicate. “coecon” refers to a negative control of HUCs transfected with lentivirus overexpression. “Coeconl” refers to the LPS-induced IC/BPS model of the negative control. “Coe” refers to the overexpression of Circ.5863, while “Coel” refers to the LPS-induced IC/BPS model after overexpression of Circ.5863.

as a competitive endogenous RNA (ceRNA) that competes with miRNAs for binding sites, thereby relieving the suppressive effect of miRNAs on target genes and subsequently upregulating their expression [6]. After validating the sequencing results by qPCR, we observed a significant downregulation of Circ.5853 expression.

Subsequently, we overexpressed Circ.5853 via lentiviral transfection and found that it could reduce inflammation damage and restore barrier function in IC/BPS, as confirmed by qPCR. Western blotting results indicate that overexpression of circ.5863 can significantly down-regulate the expression of TNF- α , IL-6, IL-1 β , and effectively alleviate inflammation in IC/BPS. According to a previous study [19], the inhibition of miR-20b-5p has been shown to decrease inflammation. Our prediction results indicate a potential interaction between circ.5863 and miR-20b-5p. When circ.5863 is overexpressed, it may function as a molecular sponge for miR-20b-5p, leading to the suppression of miR-20b-5p expression and subsequently reducing the level of inflammation.

MiRNA molecules are small, evolutionarily conserved molecules ranging in length from 18 to 25 nucleotides [20]. Multiple studies have confirmed the link between miRNAs and various diseases, including cancer, diabetes, heart disease, autoimmune disease, and more [6, 20]. In a microarray analysis of miRNA in the GSE11783, Liu et al. identified numerous DE miRNAs and DE mRNAs between ulcerative IC/PBS and control groups, suggesting their potential involvement in the early detection and progression of IC/BPS [21]. Our qPCR results indicated a statistically significant increase in hsa-miR-486-3P and hsa-miR-20b-5P, which is consistent with the sequencing results, and their stability and tissue specificity suggest their potential as biomarkers for IC/BPS [20]. Interestingly, hsa-miR-486-3p has also been implicated in epithelial-mesenchymal transformation in pulmonary fibrosis, which could be a contributing factor in the pathogenesis of IC/BPS [22]. Their findings highlight the importance of miRNAs in the development of IC/BPS and suggest new avenues for research.

Moreover, IFIT3 plays a vital role in antiviral innate immunity [23], and as human polyomavirus-2 has been detected in the urinary samples of individuals diagnosed with IC/BPS [13], further research is necessary to confirm the significance of IFIT3 in IC/BPS. Overall, our findings shed light on potential mechanisms underlying IC/BPS and suggest promising avenues for future research.

While our study sheds light on the circRNA-miRNA-mRNA network of IC/BPS, it is important

to acknowledge its limitations. The sample size was not extensive, and exploring a wider range of molecules is crucial. Additionally, bioinformatics analysis alone cannot provide complete insights, animal experiments and a more in-depth investigation of the specific mechanism of circ.5863 are necessary to confirm the significance of the regulatory network. To better understand IC/BPS and develop effective treatments, future studies should utilize larger sample sizes and more comprehensive molecular profiling.

CONCLUSION

To summarize, our study successfully established a circRNA-miRNA-mRNA network, identified IFIT3 and RSAD2 as hub genes, and found that circ.5863 can reduce inflammation damage in IC/BPS. Investigating the downstream molecular functions and pathways of these genes could reveal potential treatment-related targets and biomarkers for IC/BPS. Further research in this field is imperative to enhance our understanding of the underlying mechanisms of IC/BPS and facilitate the development of efficacious interventions.

METHODS

Sample collection

The main aim of this study was to explore new biomarkers and possible therapeutic targets for IC/BPS. Human research was approved by the Medical Ethics Committee of West China Hospital, Sichuan University (#2019186). Three IC/BPS patients who underwent cystectomy at the Department of Urology of West China Hospital at Sichuan University from July 2018 to December 2019 were included in the study. The two control patients comprised female patients with a diagnosis of pure stress urinary incontinence (PSUI) and stable bladder function, who were admitted for anti-incontinence surgery. During the assessment of bladder injuries, control samples were obtained from these patients by performing transurethral resection of the bladder after sling procedures. Full-thickness bladder tissues were collected from five participants, immediately frozen, and preserved at -80°C until further use. Supplementary Table 1 presents the inclusion and exclusion criteria utilized for IC/BPS patients. Supplementary Table 2 presents the characteristics of three IC/BPS patients and two PSUI patients.

Constructing sample library for sequence

A miRNA extraction kit (Cat #TR205-200, Tanmo) was utilized to extract total RNA from the collected tissues in accordance with the guidelines provided

by the manufacturer. The quality of RNA was determined using an Agilent Bioanalyzer 2100 (Agilent Technologies, Santa Clara, CA, USA) to obtain a RIN number. The qualified total RNA was purified with the RNAClean XP Kit (Cat A63987, Beckman Coulter, Inc., Brea, CA, USA) and treated with the RNase-Free DNase Set (Cat #79254, QIAGEN, Venlo, The Netherlands) to remove any trace of genomic DNA. After purification, the RNA underwent a series of steps, including rRNA removal, fragmentation, first-strand cDNA synthesis, second-strand cDNA synthesis, end repair, 3' end plus A, ligation linker, enrichment, and other processes, to create the sequencing sample library.

Sequencing the constructed library of cDNA

Next Generation Sequencing technology (Illumina HiSeq 2000/2500, Miseq) was used by Shanghai Bohao Biotechnology to sequence cDNA, followed by base identification and error filtering to obtain clean reads. Then, seqtk was utilized to process the clean reads and remove unqualified reads with sequencing primers, low sequencing quality, and low-end quality.

Identification of DECircRNAs

After completing the previous steps, the reference genome (GRCh38) was aligned using BWA-MEM [24] with default settings for the reads to perform further analysis, and CIRI [25] was employed to predict circRNAs. To differentiate between novel and known circRNAs based on their position information, the identified circRNAs were compared to the circBase (<http://circrna.org/>) database. By applying the thresholds of $|\log_2(\text{fold-change})| \geq 2$ and adjusted P -value ≤ 0.05 , EdgeR [26] analysis was conducted to determine the DECircRNAs.

Identification of DEMiRNAs

The constructed sequencing sample library was sequenced on the Illumina HiSeq machine to obtain raw reads, which were subsequently filtered to obtain clean reads suitable for data analysis. Fastx (version: 0.0.13) was utilized to remove unqualified reads. Subsequently, Bowtie [27] was used to compare the clean reads ranging from 18–40 nt to the GRCh38 to identify miRNAs and other small RNAs based on the position information of known miRNAs in miRBase [28] and other ncRNAs. The sRNA Toolkit software package [29] was utilized to predict novel miRNAs. By applying the thresholds of $|\log_2(\text{fold-change})| \geq 2$ and adjusted P -value ≤ 0.05 , EdgeR analysis was conducted to determine the DEMiRNAs.

Identification of DEMRNAs

After constructing the sequencing library, the spliced mapping algorithm of Hisat2 (version: 2.0.4) [30] was utilized to map clean reads to the GRCh38 genome. The reads were then normalized for gene expression analysis through conversion to Fragments Per Kilobase of exon model per Million mapped (FPKM) reads, as described in [31]. By applying the thresholds of $|\log_2(\text{fold-change})| \geq 2$ and adjusted P -value ≤ 0.05 , EdgeR analysis was conducted to determine the DEMRNAs.

GO and KEGG pathway analysis

Protein-coding genes that match the genome location of DECircRNAs, referred to as DECircRNAs parental genes, were obtained based on the position information of the circRNAs. Furthermore, we predicted the genes targeted by the DEMiRNAs by analyzing the binding of DEMiRNAs to the 3' untranslated regions of mRNA using miRanda (<http://www.mirdb.org/>) [32]. To evaluate functional enrichment, Gene Ontology (GO) analysis and Kyoto Encyclopedia of Genes and Genomes (KEGG) pathway analysis were utilized using the Database for Annotation, Visualization, and Integration Discovery (DAVID) on the parental genes of DECircRNAs, target genes of DEMiRNAs, DEMRNAs, and genes that intersect DECircRNAs parental gene with DEMRNAs [33]. We set the thresholds at $P < 0.05$ and reported the top 30 enriched pathways.

Establish a circRNA–miRNA–mRNA network

The miRNAs targeted by DECircRNAs were predicted through analyzing the circRNA sequencing data obtained using the miRanda website tool (<http://www.mirdb.org/>) [34].

Our final set of circRNAs was derived from overlapping miRNAs in the miRanda and DEMiRNAs. The interactions between miRNA and mRNA were predicted using miRanda and then intersect with DEMRNAs. The network was established, integrating candidate target mRNAs and intersecting DECircRNA-predicted miRNAs with corresponding DEMiRNAs. The network was visualized by using Cytoscape software (Version 3.7.1).

Building the PPI network and pinpointing the hub genes

To unravel the protein-protein interaction (PPI) network of the DEMRNAs, we employed the STRING database, a powerful tool for exploring functional associations between proteins, available at <http://string-db.org/> [35]. Cytoscape 3.7.1 and the cytoHubba app was utilized to

pinpoint the hub genes, which are considered the key players in the intricate network of interactions.

Cellular cultivation and transfection

HUCs (human urothelial cells) sourced from the ATCC CRL-9520 cell line were nurtured in F12K (10% fetal calf serum, 100 µg/ml streptomycin, 100 U/ml penicillin, Hyclone, USA) under optimal conditions of 37°C, 95% air, and 5% CO₂. The lentiviral vector GV689 (CMV-circRNA-EF1a-ZsGreen1-T2A-puromycin) obtained from Shanghai GeneChem, China was used to insert the synthesized sequences inducing the overexpression of circ.5863 (Supplementary Table 3). The optimal multiplicity of infection (MOI) index was 100 (Supplementary Figure 1).

Lipopolysaccharide-induced IC/BPS model

In order to construct a cellular model for IC/BPS, HUCs were subjected to incubation with 50 µg/ml of lipopolysaccharide (LPS, L2880) for 24 hours, using a well-established method to induce inflammation [36].

Quantitative polymerase chain reaction

Bio-Rad CFX Manager™ software (version 3.1) with a Bio-Rad CFX96 instrument was used to perform quantitative polymerase chain reaction (qPCR), and the qPCR primers used are listed in Supplementary Table 4. In brief, the QIAGEN kit (No. 74104, No. 1038703) was applied to extract the circRNA, total RNA, and miRNA. cDNAs were synthesized using Vazyme (R323-01-AB, R323-01-AD). Then the cDNA, cyber green (Vazyme, Q712-02-AA), and primers were mixed in the 96-well plate before preparation for qPCR procedure. The $2^{-\Delta\Delta C_t}$ method was used to calculate the relative gene expression, with GAPDH and U6 serving as internal controls. All assays were conducted in triplicate with three technical replicates per sample.

Western blotting

RIPA Lysis and Extraction Buffer (Beyotime Biotechnology, China) was used to disrupt HUCs to extract proteins. Subsequently, the protein concentration was ascertained utilizing the BCA Protein Assay Kit (Beyotime Biotechnology). Following separation using 4–20% SDS-PAGE, the protein samples were transferred to PVDF membranes (Millipore, Billerica, MA, USA). The 5% BSA Blocking Buffer was then applied to the membrane and incubated at room temperature for 1.5 hours. Subsequently, the membrane was subjected to overnight incubation at 4°C with primary antibodies against IL-1β (1:1000; AF5103, Affinity, USA), ZO-1 (1:1000; AF5145, Affinity), E-cadherin (1:1000; AF0131,

Affinity), IL-6 (1:1000; A22222, Abclonal, USA), TNF-α (1:1000; ER1919-22, Huabio, USA), and GAPDH (1:5000; ab181602, Abcam, UK). Following that, the HRP-conjugated secondary antibodies (1:5000) were applied to the membrane and allowed to bind specifically to their corresponding protein targets during a 1.5-hour incubation at room temperature. Enhanced chemiluminescence (Thermo Fisher Scientific, Waltham, MA, USA) was then employed to visualize the proteins, generating a radiant glow upon interaction. The resulting bands were captured and their intensities were quantified using the ChemiDoc MP Imaging System (Bio-Rad, Hercules, CA, USA), enabling assessment of protein abundance or expression levels.

Statistical analysis

GraphPad Prism (version 9.5) was utilized for statistical analysis, and the results were expressed as mean ± SD. For intergroup comparisons, a two-tailed Student's *t*-test was employed, while multigroup comparisons were performed using one-way ANOVA. The threshold for statistical significance was defined as $P < 0.05$.

Data availability statement

The data supporting the finding of this article are available from the corresponding author.

Abbreviations

IC/BPS: Interstitial cystitis/bladder pain syndrome; PPI: protein-protein interaction; circRNA: Circular RNA; EMT: epithelial-mesenchymal transition; DEcircRNAs: CircRNAs exhibiting differential expression; DEmiRNAs: miRNAs exhibiting differential expression; DEMRNAs: mRNAs exhibiting differential expression; FPKM: Fragments Per Kilobase of exon model per Million mapped; GO: Gene Ontology; KEGG: Kyoto Encyclopedia of Genes and Genomes; DAVID: Database for Annotation, Visualization, and Integration Discovery; HUCs: human urothelial cells; LPS: Lipopolysaccharide; qPCR: quantitative polymerase chain reaction; PSUI: pure stress urinary incontinence.

AUTHOR CONTRIBUTIONS

Conceptualization, Shiqin Yang and Liao Peng; Formal analysis, Shiqin Yang, Liao Peng, Ledu Lin, Yuanzhuo Chen, Mengzhu Liu and Jiawei Chen; Funding acquisition, Deyi Luo; Methodology, Shiqin Yang, Liao Peng and Chi Zhang; Project administration, Deyi Luo; Software, Shiqin Yang, Liao Peng, Ledu Lin and Yuanzhuo Chen; Supervision, Deyi Luo; Validation, Shiqin Yang, Ledu Lin and Mengzhu Liu; Writing – original draft, Shiqin Yang, Liao Peng, Ledu Lin,

Yuanzhuo Chen, Mengzhu Liu, Chi Zhang and Jiawei Chen; Writing – review and editing, Deyi Luo.

CONFLICTS OF INTEREST

The authors declare no conflicts of interest related to this study.

ETHICAL STATEMENT AND CONSENT

All subjects gave their informed consent for inclusion before they participated in the study. The study was conducted in accordance with the Declaration of Helsinki, and the protocol was approved by the Ethics Committee of West China Hospital, Sichuan University (#2019186).

FUNDING

This study was funded by the National Natural Science Fund of China (Grant Nos. 81770673 and 32171301).

REFERENCES

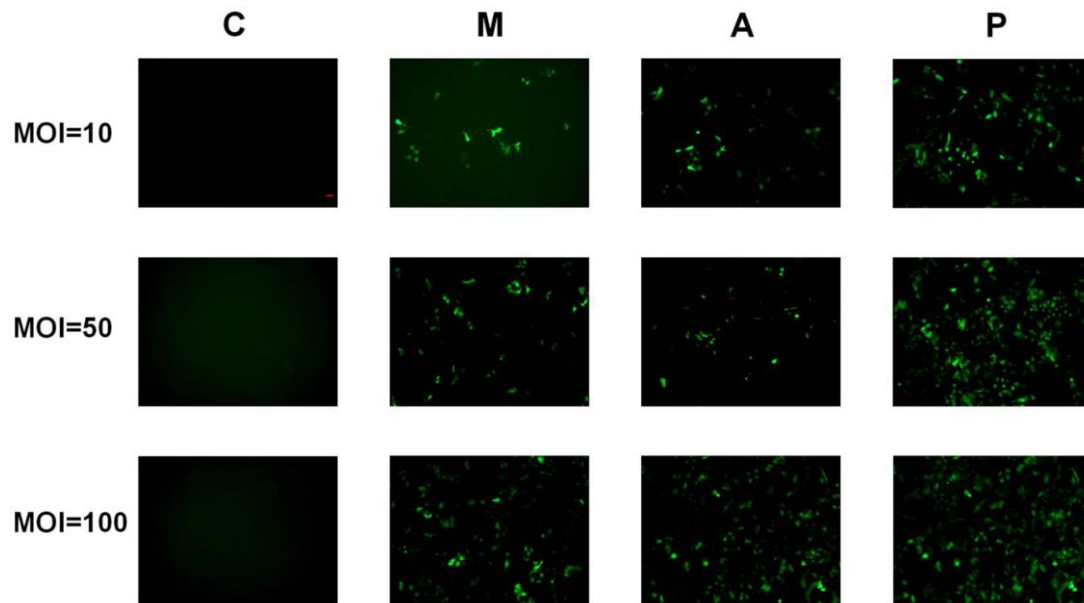
1. Campbell-Walsh-Wein Urology, vol. II, 12 edn. USA: Elsevier, Philadelphia, PA19103-2899. 2021.
2. Berry SH, Elliott MN, Suttrop M, Bogart LM, Stoto MA, Eggers P, Nyberg L, Clemens JQ. Prevalence of symptoms of bladder pain syndrome/interstitial cystitis among adult females in the United States. *J Urol.* 2011; 186:540–4. <https://doi.org/10.1016/j.juro.2011.03.132> PMID:21683389
3. Whitmore KE, Fall M, Sengiku A, Tomoe H, Logadottir Y, Kim YH. Hunner lesion versus non-Hunner lesion interstitial cystitis/bladder pain syndrome. *Int J Urol.* 2019 (Suppl 1); 26:26–34. <https://doi.org/10.1111/iju.13971> PMID:31144757
4. Jeck WR, Sorrentino JA, Wang K, Slevin MK, Burd CE, Liu J, Marzluff WF, Sharpless NE. Circular RNAs are abundant, conserved, and associated with ALU repeats. *RNA.* 2013; 19:141–57. <https://doi.org/10.1261/rna.035667.112> PMID:23249747
5. Guo JU, Agarwal V, Guo H, Bartel DP. Expanded identification and characterization of mammalian circular RNAs. *Genome Biol.* 2014; 15:409. <https://doi.org/10.1186/s13059-014-0409-z> PMID:25070500
6. Hansen TB, Jensen TI, Clausen BH, Bramsen JB, Finsen B, Damgaard CK, Kjems J. Natural RNA circles function as efficient microRNA sponges. *Nature.* 2013; 495:384–8. <https://doi.org/10.1038/nature11993> PMID:23446346
7. Memczak S, Jens M, Elefsinioti A, Torti F, Krueger J, Rybak A, Maier L, Mackowiak SD, Gregersen LH, Munschauer M, Loewer A, Ziebold U, Landthaler M, et al. Circular RNAs are a large class of animal RNAs with regulatory potency. *Nature.* 2013; 495:333–8. <https://doi.org/10.1038/nature11928> PMID:23446348
8. Beermann J, Piccoli MT, Viereck J, Thum T. Non-coding RNAs in Development and Disease: Background, Mechanisms, and Therapeutic Approaches. *Physiol Rev.* 2016; 96:1297–325. <https://doi.org/10.1152/physrev.00041.2015> PMID:27535639
9. Gu Y, Ke G, Wang L, Zhou E, Zhu K, Wei Y. Altered Expression Profile of Circular RNAs in the Serum of Patients with Diabetic Retinopathy Revealed by Microarray. *Ophthalmic Res.* 2017; 58:176–84. <https://doi.org/10.1159/000479156> PMID:28817829
10. Jiang C, Xu M, Zhu J, Yang D, Xue B. CircTHBS1 facilitates the progression of interstitial cystitis depending on the regulation of miR-139-5p/MFN2 axis. *Drug Dev Res.* 2022; 83:351–61. <https://doi.org/10.1002/ddr.21864> PMID:34368980
11. Song YJ, Cao JY, Jin Z, Hu WG, Wu RH, Tian LH, Yang B, Wang J, Xiao Y, Huang CB. Inhibition of microRNA-132 attenuates inflammatory response and detrusor fibrosis in rats with interstitial cystitis via the JAK-STAT signaling pathway. *J Cell Biochem.* 2019; 120:9147–58. <https://doi.org/10.1002/jcb.28190> PMID:30582204
12. Gheinani AH, Akshay A, Besic M, Kuhn A, Keller I, Bruggmann R, Rehrauer H, Adam RM, Burkhard FC, Monastyrskaya K. Integrated mRNA-miRNA transcriptome analysis of bladder biopsies from patients with bladder pain syndrome identifies signaling alterations contributing to the disease pathogenesis. *BMC Urol.* 2021; 21:172. <https://doi.org/10.1186/s12894-021-00934-0> PMID:34876093
13. Peng L, Jin X, Li BY, Zeng X, Liao BH, Jin T, Chen JW, Gao XS, Wang W, He Q, Chen G, Gong LN, Shen H, et al. Integrating single-cell RNA sequencing with spatial transcriptomics reveals immune landscape for interstitial cystitis. *Signal Transduct Target Ther.* 2022; 7:161. <https://doi.org/10.1038/s41392-022-00962-8> PMID:35589692

14. Hanno PM, Erickson D, Moldwin R, Faraday MM, and American Urological Association. Diagnosis and treatment of interstitial cystitis/bladder pain syndrome: AUA guideline amendment. *J Urol.* 2015; 193:1545–53.
<https://doi.org/10.1016/j.juro.2015.01.086>
PMID:[25623737](https://pubmed.ncbi.nlm.nih.gov/25623737/)
15. Xue C, Li G, Zheng Q, Gu X, Bao Z, Lu J, Li L. The functional roles of the circRNA/Wnt axis in cancer. *Mol Cancer.* 2022; 21:108.
<https://doi.org/10.1186/s12943-022-01582-0>
PMID:[35513849](https://pubmed.ncbi.nlm.nih.gov/35513849/)
16. Chen M, Lai X, Wang X, Ying J, Zhang L, Zhou B, Liu X, Zhang J, Wei G, Hua F. Long Non-coding RNAs and Circular RNAs: Insights Into Microglia and Astrocyte Mediated Neurological Diseases. *Front Mol Neurosci.* 2021; 14:745066.
<https://doi.org/10.3389/fnmol.2021.745066>
PMID:[34675776](https://pubmed.ncbi.nlm.nih.gov/34675776/)
17. Altesha MA, Ni T, Khan A, Liu K, Zheng X. Circular RNA in cardiovascular disease. *J Cell Physiol.* 2019; 234:5588–600.
<https://doi.org/10.1002/jcp.27384>
PMID:[30341894](https://pubmed.ncbi.nlm.nih.gov/30341894/)
18. Gao Y, Shang S, Guo S, Li X, Zhou H, Liu H, Sun Y, Wang J, Wang P, Zhi H, Li X, Ning S, Zhang Y. Lnc2Cancer 3.0: an updated resource for experimentally supported lncRNA/circRNA cancer associations and web tools based on RNA-seq and scRNA-seq data. *Nucleic Acids Res.* 2021; 49:D1251–8.
<https://doi.org/10.1093/nar/gkaa1006>
PMID:[33219685](https://pubmed.ncbi.nlm.nih.gov/33219685/)
19. Liu J, Liu Y, Zhang L, Chen Y, Du H, Wen Z, Wang T, Chen D. Down-regulation of circDMNT3B is conducive to intestinal mucosal permeability dysfunction of rats with sepsis via sponging miR-20b-5p. *J Cell Mol Med.* 2020; 24:6731–40.
<https://doi.org/10.1111/jcmm.15324>
PMID:[32383354](https://pubmed.ncbi.nlm.nih.gov/32383354/)
20. Zhang Y, Ding Y, Li M, Yuan J, Yu Y, Bi X, Hong H, Ye J, Liu P. MicroRNA-34c-5p provokes isoprenaline-induced cardiac hypertrophy by modulating autophagy via targeting ATG4B. *Acta Pharm Sin B.* 2022; 12:2374–90.
<https://doi.org/10.1016/j.apsb.2021.09.020>
PMID:[35646533](https://pubmed.ncbi.nlm.nih.gov/35646533/)
21. Liu S, Feng S, Luo D. Analysis of key genes and micro-RNA-mRNA regulatory networks in women with ulcerative interstitial cystitis/pain bladder syndrome. *Int Urogynecol J.* 2019; 30:1487–95.
<https://doi.org/10.1007/s00192-018-3817-x>
PMID:[30456462](https://pubmed.ncbi.nlm.nih.gov/30456462/)
22. Yan Z, Ao X, Liang X, Chen Z, Liu Y, Wang P, Wang D, Liu Z, Liu X, Zhu J, Zhou S, Zhou P, Gu Y. Transcriptional inhibition of miR-486-3p by BCL6 upregulates Snail and induces epithelial-mesenchymal transition during radiation-induced pulmonary fibrosis. *Respir Res.* 2022; 23:104.
<https://doi.org/10.1186/s12931-022-02024-7>
PMID:[35484551](https://pubmed.ncbi.nlm.nih.gov/35484551/)
23. Zhang W, Li Y, Xin S, Yang L, Jiang M, Xin Y, Wang Y, Cao P, Zhang S, Yang Y, Lu J. The emerging roles of IFIT3 in antiviral innate immunity and cellular biology. *J Med Virol.* 2023; 95:e28259.
<https://doi.org/10.1002/jmv.28259>
PMID:[36305096](https://pubmed.ncbi.nlm.nih.gov/36305096/)
24. Li H. Aligning sequence reads, clone sequences and assembly contigs with BWA-MEM. *Eprint Arxiv.* 2013.
<https://doi.org/10.48550/arXiv.1303.3997>
25. Gao Y, Wang J, Zhao F. CIRI: an efficient and unbiased algorithm for de novo circular RNA identification. *Genome Biol.* 2015; 16:4.
<https://doi.org/10.1186/s13059-014-0571-3>
PMID:[25583365](https://pubmed.ncbi.nlm.nih.gov/25583365/)
26. Robinson MD, McCarthy DJ, Smyth GK. edgeR: a Bioconductor package for differential expression analysis of digital gene expression data. *Bioinformatics.* 2010; 26:139–40.
<https://doi.org/10.1093/bioinformatics/btp616>
PMID:[19910308](https://pubmed.ncbi.nlm.nih.gov/19910308/)
27. Langmead B, Trapnell C, Pop M, Salzberg SL. Ultrafast and memory-efficient alignment of short DNA sequences to the human genome. *Genome Biol.* 2009; 10:R25.
<https://doi.org/10.1186/gb-2009-10-3-r25>
PMID:[19261174](https://pubmed.ncbi.nlm.nih.gov/19261174/)
28. Kozomara A, Griffiths-Jones S. miRBase: annotating high confidence microRNAs using deep sequencing data. *Nucleic Acids Res.* 2014; 42:D68–73.
<https://doi.org/10.1093/nar/gkt1181>
PMID:[24275495](https://pubmed.ncbi.nlm.nih.gov/24275495/)
29. Stocks MB, Moxon S, Mapleson D, Woolfenden HC, Mohorianu I, Folkes L, Schwach F, Dalmay T, Moulton V. The UEA sRNA workbench: a suite of tools for analysing and visualizing next generation sequencing microRNA and small RNA datasets. *Bioinformatics.* 2012; 28:2059–61.
<https://doi.org/10.1093/bioinformatics/bts311>
PMID:[22628521](https://pubmed.ncbi.nlm.nih.gov/22628521/)
30. Kim D, Langmead B, Salzberg SL. HISAT: a fast spliced aligner with low memory requirements. *Nat Methods.* 2015; 12:357–60.
<https://doi.org/10.1038/nmeth.3317>
PMID:[25751142](https://pubmed.ncbi.nlm.nih.gov/25751142/)

31. Mortazavi A, Williams BA, McCue K, Schaeffer L, Wold B. Mapping and quantifying mammalian transcriptomes by RNA-Seq. *Nat Methods*. 2008; 5:621–8.
<https://doi.org/10.1038/nmeth.1226>
PMID:[18516045](https://pubmed.ncbi.nlm.nih.gov/18516045/)
32. Wong N, Wang X. miRDB: an online resource for microRNA target prediction and functional annotations. *Nucleic Acids Res*. 2015; 43:D146–52.
<https://doi.org/10.1093/nar/gku1104>
PMID:[25378301](https://pubmed.ncbi.nlm.nih.gov/25378301/)
33. Huang da W, Sherman BT, Lempicki RA. Systematic and integrative analysis of large gene lists using DAVID bioinformatics resources. *Nat Protoc*. 2009; 4:44–57.
<https://doi.org/10.1038/nprot.2008.211>
PMID:[19131956](https://pubmed.ncbi.nlm.nih.gov/19131956/)
34. Dudekula DB, Panda AC, Grammatikakis I, De S, Abdelmohsen K, Gorospe M. CirInteractome: A web tool for exploring circular RNAs and their interacting proteins and microRNAs. *RNA Biol*. 2016; 13:34–42.
<https://doi.org/10.1080/15476286.2015.1128065>
PMID:[26669964](https://pubmed.ncbi.nlm.nih.gov/26669964/)
35. Szklarczyk D, Morris JH, Cook H, Kuhn M, Wyder S, Simonovic M, Santos A, Doncheva NT, Roth A, Bork P, Jensen LJ, von Mering C. The STRING database in 2017: quality-controlled protein-protein association networks, made broadly accessible. *Nucleic Acids Res*. 2017; 45:D362–8.
<https://doi.org/10.1093/nar/gkw937>
PMID:[27924014](https://pubmed.ncbi.nlm.nih.gov/27924014/)
36. Silberfeld A, Chavez B, Obidike C, Daugherty S, de Groat WC, Beckel JM. LPS-mediated release of ATP from urothelial cells occurs by lysosomal exocytosis. *NeuroUrol Urodyn*. 2020; 39:1321–9.
<https://doi.org/10.1002/nau.24377>
PMID:[32374925](https://pubmed.ncbi.nlm.nih.gov/32374925/)

SUPPLEMENTARY MATERIALS

Supplementary Figure



Supplementary Figure 1. Lentiviral transduction. C stands for control group, M stands for transduction with lentivirus only, A stands for transduction with lentivirus and enhanced infection reagent A, P stands for transduction with lentivirus and enhanced infection reagent P.

Supplementary Tables

Supplementary Table 1. Inclusion and exclusion criteria of the patients with interstitial cystitis.

Inclusion criteria	
1.	Patients over 18 years old;
2.	Previously diagnosed of interstitial cystitis more than 6 months;
3.	The characteristic pathological findings in the bladder wall were identified by cystoscopy;
4.	O’Leary-Sant Interstitial Cystitis Symptom and Problem Index score over 18;
5.	Patients are aware of the purpose of this study and give fully informed consent;
Exclusion criteria	
1.	General conditions
1.	Currently diagnosed with cancer, severe heart, lung, liver, kidney, or blood disorder.
2.	Patients who are pregnant or desire to become pregnant.
3.	The investigators assessed that the patient was not suitable for the study.
2.	Urological problems
1.	Have previous history of urinary infection (e.g., bacterial cystitis) within 12 weeks;
2.	Currently diagnosed with Urethral diseases (e.g., urethral stone, bladder cancer); Gynaecological diseases (e.g., pelvic organ prolapse) or neurogenic urinary frequency
3.	Patients accompanied by urinary tract symptoms (i.e., bladder pain, urinary frequency and/or urinary urgency)
4.	Have previous history of augmentation cystoplasty or cystectomy;
3.	Treatment related
1.	Have history of the following therapies within 24 weeks: Hydrodistension, intravesical laser therapy, intravesical electrical coagulation, transurethral resection, pelvic reconstructive surgery, nerve block or spinal cord stimulation for pain relief;
2.	Received intravesical instillation of drugs within 12 weeks.
3.	Have previous history of chemical compound (such as cyclophosphamide) derived cystitis.

Supplementary Table 2. The characteristics of IC/BPS patients and PSUI patients.

Diagnosis	Age (years)	BMI	Duration (months)	Menopause	Hypertension	DM	Voids/day	Night urination	ICSI	ICPI	VAS
IC/BPS-1	58	23.44	11.0	Post	0	0	20	4	18	16	9
IC/BPS-2	56	23.35	52.0	Post	0	0	21	5	17	14	8
IC/BPS-3	60	22.22	24.0	Post	0	0	21	9	16	15	3
PSUI-1	67	19.25	–	Post	0	0	5	0	0	0	0
PSUI-2	68	24.51	–	Post	0	0	6	0	0	0	0

Abbreviations: BMI: body mass index (kg/m²); DM: diabetes mellitus; IC: interstitial cystitis/bladder pain syndrome; PSUI: pure stress urinary incontinence; ICSI: ICPI interstitial cystitis symptom index and problem index; VAS: visual analogue scale.

Supplementary Table 3. The sequence of circ.5863 transferred by transfection.

circRNA.5863
 AAAAAGACCTTGGGGTAGAGGGGCGCCACGAGAGGCGGGTCTGGCGCTGACATCCAACCCCGTGCCCCCTCC
 CTGCAGGATGCTGGTGGACTGTGTGCCCTGGTGGAGGTGGACGACATGATGATCATGGGCAAGAAGCCTGA
 CCCC*ATGGCAGTGGCAGCACCATGATGCAAACCAAGACCTTCTCCTCTTCTCCTCATCCAAGAAGATGG
 GCAGGTGAGCACCAGCACCAATCCCTGACCATAGAGGAGTCAGTGCCACAGGGGACCTAACTGCAAACCCG
 TTTACAGAGG

Supplementary Table 4. Sequence information of primers.

Primers	Sequences (5'–3')
TNF- α	F: GCTGCACTTTGGAGTGATCG R: GCTTGAGGGTTTGCTACAACA
IL-1 β	F: AGCTCGCCAGTGAAATGATG R: GACATGGAGAACACCACTTGT
GAPDH	F: ACAACTTTGGTATCGTGGAAGG R: GCCATCACGCCACAGTTTC
ZO-1	F: CAACATACAGTGACGCTTCACA R: CACTATTGACGTTTCCCCTC
E-Cadherin	F: GGATGTGAATGAAGCCCCCA R: AGTGGAATGGCACCAGTGT
IL-6	F: CCTGAACCTTCCAAAGATGGC R: TTCACCAGGCAAGTCTCCTCA
Circ.5863	F: ATCCAAGAAGATGGGCAGGTG R: GGGTTTGCAGTTAGGTCCCC
Circ.8045	F: GGGAATGCGTCATCACCGAG R: TGTATGGCACATCCTTTGGCT
Circ.8742	F: AGGTCTGGAAAGCATGGAAAT R: AGTTCAAACATGAAAAGAGTCCAT
miR-134-5p	F: GCCGAGGGGGAGACCAGUUG R: CTCAACTGGTGTCTGTGGA
miR-136-5p	F: ACTCCATTTGTTTTGATGATGGA R: GCAGGGTCCGAGGTATTC
miR-20b-5p	F: CGCCATCAAAGTGCTCATAGTGC R: ATCCAGTGCAGGGTCCGAGG
miR-106a-5p	F: TGCAGTAGATCTCAAAAAGCTACC R: CCTTGGCCATGTAAAAGTGC
miR-486-3p	F: GGGGCAGCTCAGTACA R: GGTCCAGTTTTTTTTTTTTTTTTTTTTTTTACCT
U6	F: CTCGCTTCGGCAGCAC R: AACGCTTCACGAATTTGCGT